MAGNETIC FLUX LEAKAGE INVESTIGATION OF INTERACTING DEFECTS: COMPETITIVE EFFECTS OF STRESS CONCENTRATION AND MAGNETIC SHIELDING

C Mandache[1,2] and L Clapham[1]
[1]Queen's University, Kingston, Ontario, K7L 3N6
[2]Present address: National Research Council, Ottawa, Ontario, Canada

The magnetic flux leakage (MFL) method is used for in-line inspection of oil and gas pipelines. Corrosion-induced MFL signals are sensitive to the level of stress and magnetic flux density existing in the pipe wall. Defects act as stress raisers, locally influencing the magnetization of the material, and subsequently the path of flux flow. Two adjacent corrosion pits can furthermore complicate this situation by the superposition of their stress concentrations and by the mutual shielding of the defects from the applied flux density. This type of defect geometry is termed *interacting defects*. In this study, various degrees of interaction were considered by modifying the separation and direction of alignment of the two defects. The MFL signals generated by these defect geometries were analyzed as a function of applied stress and magnetic flux density in the bulk material. While the overall MFL signal amplitude dependence on stress was minimized at high flux densities, it was observed that the shape of the MFL profile was dictated by the interacting defect geometry. The absolute MFL amplitude was found to be influenced by the local residual stress developed at the defect edges.

Introduction: The MFL method relies on calibration runs for correct interpretation of the leakage signals in terms of defect location, size, and depth. Calibration of the corrosion-induced MFL signals as a function of the test object and inspection tool properties had been extensively studied, as reviewed in [1]. Although the effect of stress on the magnetic properties of the pipe ferromagnetic steel is not clearly understood, the most efficient method of reducing stress influences on the MFL signals is by magnetically saturating the pipe [2], minimizing in this way local variations in the permeability of the material.

Oil and gas pipelines are operated at pressures as high as 70% of their yield strength [3]. This line pressure generates circumferential (hoop) stress in the pipe wall. Furthermore, much higher stresses are expected in the vicinity of the corrosion defects since these act as stress raisers [4,5] in the material. Three types of stresses are usually developed in a pipeline [6,7]: (i) bulk stress, occurring in the volume of the specimen as a result of the pressure of the transported fluid, (ii) local stress, generated in the neighbourhood of metal-loss defects, and (iii) residual stress, that develops in the sample after the removal of the applied load.

When clustering of the corrosion defects occurs - regions of high stress concentration and magnetic flux shielding further complicates the defect-induced MFL signal calibration [6]. The focus of this study is the interpretation of the experimental MFL features generated by interacting defects. This type of defect geometry consists of two holes that are sufficiently close to influence both stress and flux distributions in the region between them. The critical area between defects is subject to local stress concentration superposition and magnetic flux shielding. Figure 1 depicts the interacting situation most often encountered in practice: two corrosion pits, aligned along the pipe axis. Most field inspections use a magnetization of the pipe wall in the same direction [8]. In figure 1, the shaded zone experiences lower flux density than the bulk of the material, since the defects mutually shield each other from the applied magnetic field. Therefore, the semicircular part of the defect, called from now on the "inside edge", facing the other defect may be more stress-sensitive even in conditions of bulk magnetic saturation.

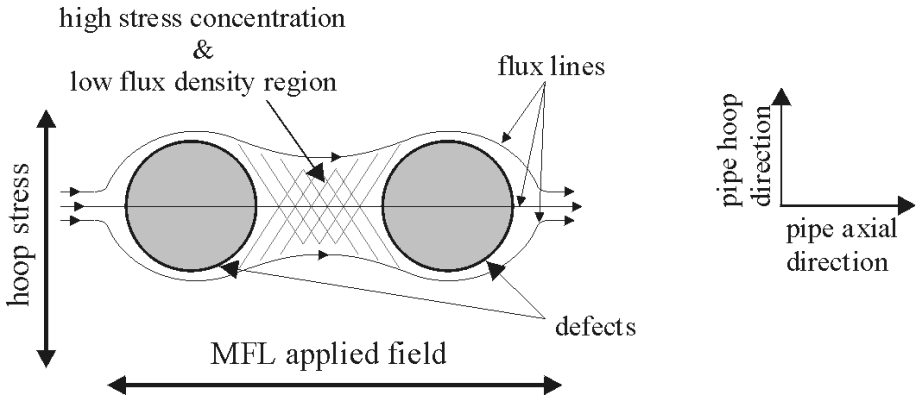

Fig. 1. Representation of two axially aligned interacting defects. The area between defects is exposed to higher stress superposition and lower-than-background magnetic flux density.

Experimental Details: The defect geometries investigated in this MFL experimental study are schematically shown in figure 2. The samples were mild steel plates 500 mm long, 216 mm wide, and 2.8 mm thick. The yield strength of the material was 291MPa, while its Young's modulus was 219 GPa. All the defects were in-situ drilled by an electrochemical milling method under bulk 'hoop' stress conditions of 135 MPa, representing 46% of the material yield strength. The artificial metal-loss defect created by electrochemical milling simulates a real corrosion process, while avoiding, at the same time, introduction of residual stresses around the defect, as it happens during the mechanical drilling. Also, all the defects examined were through-wall pits.

According to the Airy's function analytical approach [5], the stress concentration factor developed in the immediate vicinity of a hole is three times higher than the bulk stress, decreases quadratically with the distance from the defect edge, and extends for a region equal to the hole diameter. Consequently, the defect geometries were termed *weakly* or *strongly interacting* defects when their separation is equal to a hole diameter and radius, respectively. The *misaligned* defects consist in the same geometry as the strongly interacting holes, but with their direction of alignment making an angle of 45^{o} with the applied field. The elimination of the critical area between the weakly interacting defects created a new type of geometry, called here a *racetrack* defect.

An 'axial' DC magnetic field circuit containing NdFeB permanent magnets was used to generate magnetic flux densities in the samples. The flux density inside the specimen was varied by modifying the configuration of the magnetizing circuit. A Hall sensor (Honeywell, SS94A1) was used to scan an 80 mm x 80 mm area centred on the defect geometry, between the magnetic pole pieces. Stress was applied along the sample's length by clamping it in a hydraulic stress rig, while bulk strain was measured by gauges, at a location away from the defects. This applied load simulated hoop stress occurring in a pipeline as a result of pressurizing the transported fluid. This experimental setup is presented elsewhere [2,6] and simulates a realistic industrial inspection arrangement [8], with the principal stress direction (hoop) and magnetic field perpendicularly oriented.

Although both the normal ('radial') and tangential ('axial') MFL components were recorded in this study, and four applied flux densities were used (1.0 T, 1.3 T, 1.6 T, and 1.7 T), for clarity reasons, only the normal ('radial') component is analyzed here. The flux leakage sensed along the 'axial' direction provided similar results in terms of stress sensitivity of the MFL characteristics.

The parameters of interest are the amplitude of the MFL signal or its peak-to-peak value, and the MFL profile. The MFL peak-to-peak amplitude, MFL_{pp}, denotes the difference between the maximum and minimum MFL values within a surface scan. The 'radial MFL profile' feature employed in this study represents the section cutting the surface scan through the centres of the defects and aligned along the applied magnetic flux direction.

The Hall sensor was maintained at a constant lift-off above the steel plate of 1.5 mm and its scanning resolution was set equal to 1 mm on each direction of measurement.

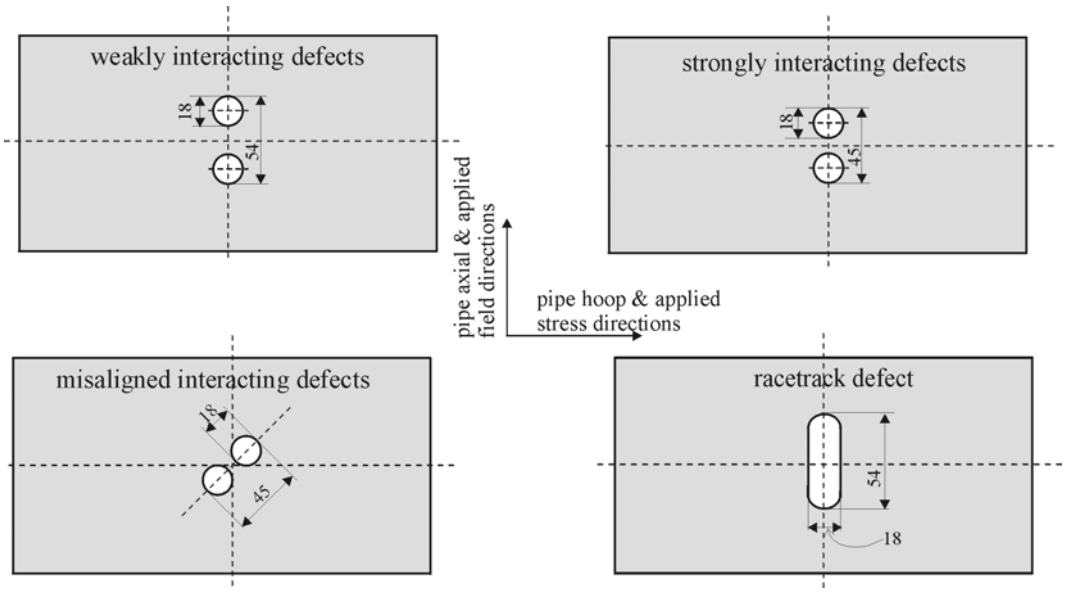

Fig. 2. Defect geometries investigated. All dimensions are given in mm

Results and Discussion: It is well known that the percentage change in the MFL signal amplitude with the applied stress is progressively minimized with the increase of the magnetic flux density in the specimen [2,3,6,7]. Therefore, in figure 3, only the smallest (1.0 T) and largest flux density (1.7 T) cases are presented.

For a flux density of 1.0 T, the MFL_{pp} percentage change, $MFL_{pp}(\%)$, is significantly influenced by the magnitude of applied stress, as seen in figure 3.a. For the highest flux density used, 1.7 T - value close to the saturation level of the specimen (~1.8-2.0 T), the bulk stress effect on MFL amplitude is less than about 5%, as shown in figure 3.b.

Comparison between the two magnetizing situations presented in figure 3 substantiates the fact that stress modifies the magnetic flux path around defects by changing the magnetic permeability. The elastic stress introduces a higher-than-background permeability or magnetic easy axis along the direction of load [6,7]. This stress-induced anisotropy facilitates a path of lower magnetic reluctance around the defects region and consequently, the magnetic field lines spread circumferentially inside the sample rather than closing through the air. Also, from the in-situ defect drilling, local plastic deformation and residual compressive stress introduced at defect edges tangential to stress were expected to lower the magnetic permeability. In the realistic situation discussed here the residual stress introduced at the defect drilling stage has a permanent contribution to subsequent inspections and the applied tensile stress superimposes over the local residual stress regions at the defect edges. The compressive residual stress and the applied tensile load have an opposite effect on the material permeability. Therefore, as a function of the residual stress magnitude, more flux lines will intersect the defect boundary and leak into the environment rather than spreading around the defects, inside the steel sample.

Due to stress superposition and closeness of the holes, higher stresses are expected to develop between the strongly interacting defects than in the case of their weakly interacting counterparts. However, in figure 3.a only small changes are observed between weakly and strongly interacting defect cases; this suggests that the stress in the area between defects has a small influence on the MFL_{pp} amplitude, and this parameter is mainly generated by the defect edges first "seen" by the magnetic field (the "outside edges" of the defects).

This supposition is tested by comparing the $MFL_{pp}(\%)$ variation with stress for the elongated defect (racetrack) with the weakly interacting defects. Both geometries have the same end-to-end dimensions and "outside edges", as schematically represented in figure 2. The results obtained for the low flux density case shown in figure 3.a are inconsistent with the idea that the stresses between defects have little effect, and prompts a more detailed analysis of the MFL characteristics.

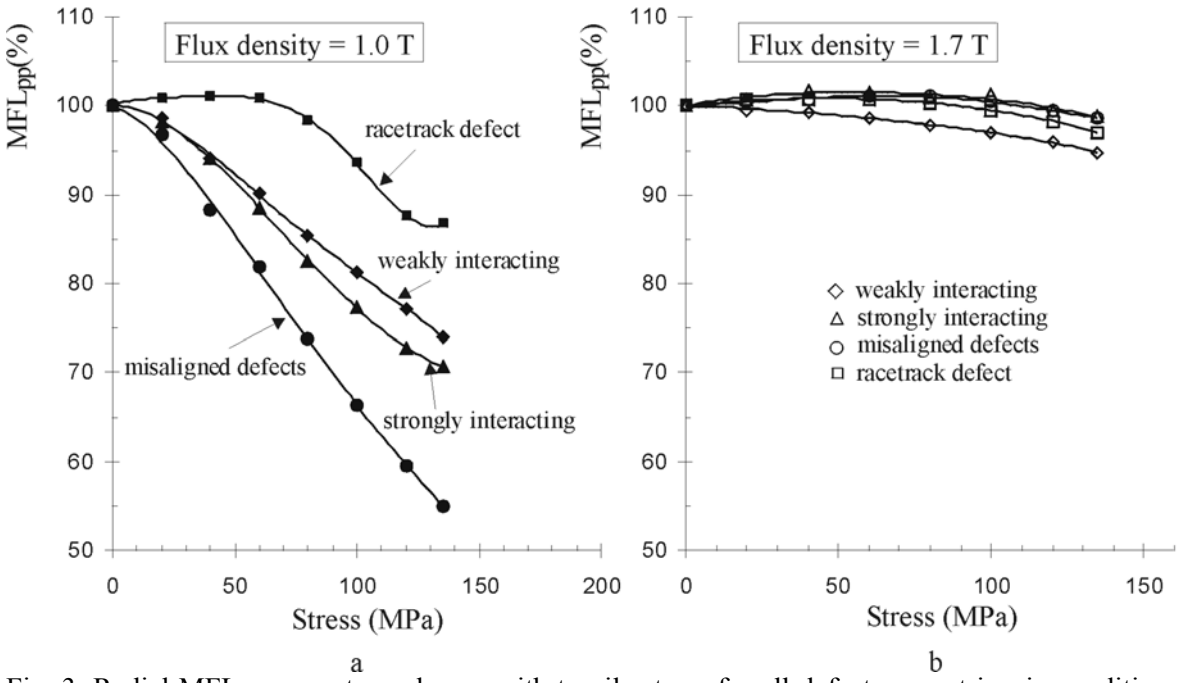

Fig. 3. Radial MFL_{pp} percentage change with tensile stress for all defect geometries, in conditions of applied flux densities of (a) 1.0 T and (b) 1.7 T.

Weakly versus strongly interacting defects:

As seen in figure 3, the relative changes in MFL_{pp}(%) as a function of applied stress for the two axially aligned interacting defect types have a similar behaviour, although their geometries correspond to different degrees of interaction. The representation of the absolute MFL_{pp} variation with stress reveals that more flux is forced out of the sample in the case of strongly interacting defects, as presented in figure 4. Compared to weakly interacting defects, this strongly interacting case has vicinity regions of higher plastic deformation due to in-situ defect drilling. This creates local compressive residual stresses in the hoop direction. As a result the magnetic easy axis direction changes locally, in the defect neighbourhood, and aligns itself perpendicular to the direction of compressive stress, i.e. along the magnetic field. This suggests that more magnetic field lines intersect the defect boundary and consequently, more flux is diverted through the air.

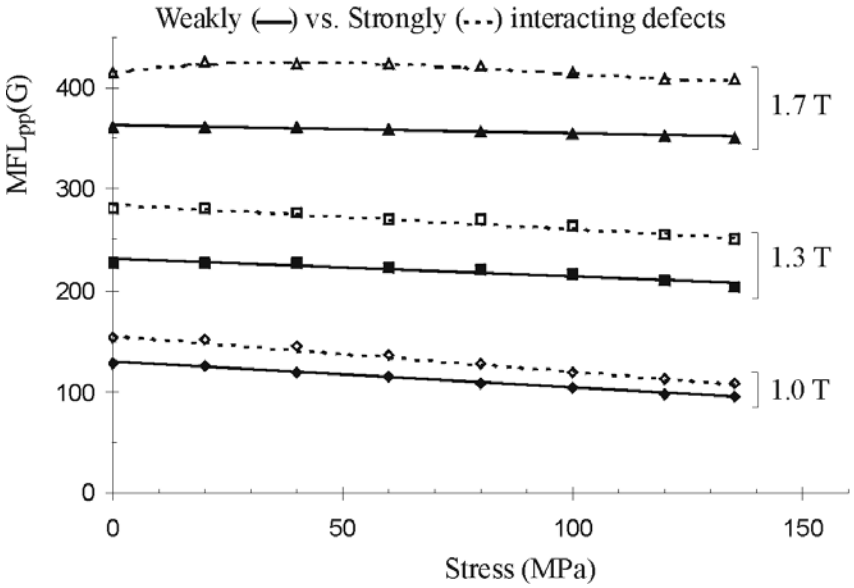

Strongly versus misaligned interacting defects:

These two types of interacting defects represent the same geometry, two similar adjacent holes, with the defect separation equal to one hole radius. The only difference lies in their direction of alignment: the strongly interacting defects are aligned along the 'axial' coordinate, the same as the orientation of the applied magnetic field, while the misaligned holes have the axis joining their centres making an angle of 45^{o} with respect to the applied field (figure 2). The orientation of the misaligned defects prevents the formation of high stress superposition regions and allows more flux to enter the area between the two holes. Overall, this translates in higher flux retentivity inside the steel plate, as observed in figure 3.a – where this type of defect exhibits the largest stress dependence of the MFL_{pp}(%) on the applied stress, and in figure 5, where the absolute MFL_{pp} value is compared to the axially aligned strongly interacting defects. Moreover, in the misaligned defects case, the holes do not shield each other (or the central region between them) from the applied magnetic field. As a note, it is interesting to observe that the plots of MFL_{pp} versus applied stress for strongly and misaligned defects have almost the same slope for each bulk flux density level (figure 5).

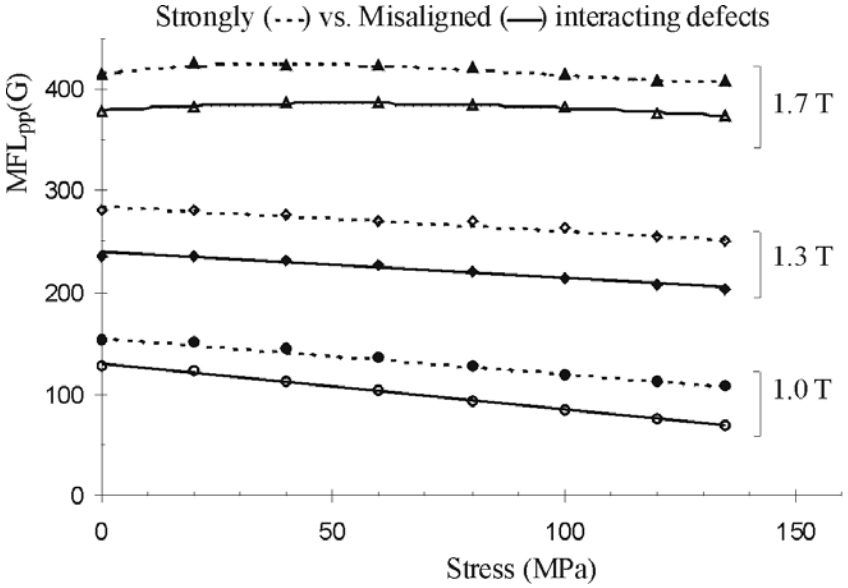

Weakly interacting versus racetrack defects:

Although these two defect geometries have the same overall dimensions and "outside" boundaries (figure 2), there were clear differences observed in their percentage MFL_{pp}(%) change variation with stress for 1.0 T flux density, as plotted in figure 3.a. Taking into account the stress concentration factors in the immediate vicinity of the defects is proportional to the ratio of length to width of the defect [4], much higher stresses were developed during the in-situ defect formation of the racetrack than in the case of weakly interacting defects. As for strongly interacting holes, discussed earlier, higher compressive residual stress at the racetrack edges changes the magnetic easy axis direction, and orients it along the racetrack length. This results in a higher local magnetic anisotropy along the applied field direction for the elongated defect, and more flux leakage at the defect boundary than in weakly interacting holes situation, as seen in figure 6.

The overall MFL stress sensitivity for the racetrack defect is much lower than for all other defects investigated, fact noticed from figure 3.a. The residual compressive stress seems to have a dominant effect in the applied stress range 0-60 MPa, when both MFL_{pp}(%) (figure 3.a) and the absolute MFL_{pp} remained almost unchanged, as indicated in figure 6. For applied stresses higher than 60 MPa, these parameters have a higher dependence on the bulk load, showing a decreasing trend with stress.

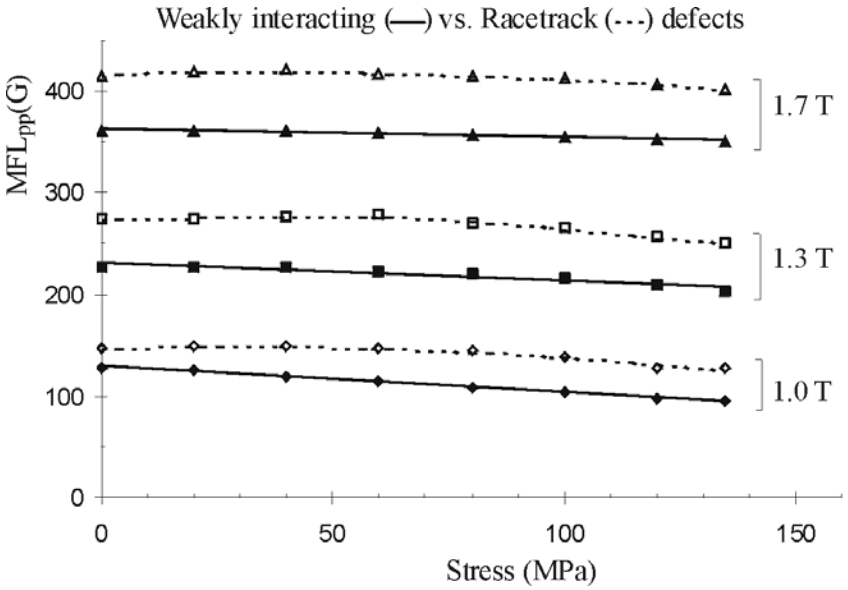

At high flux density (1.7 T), the MFL amplitude dependence on load is very small (as seen in figures 3-6), mainly due minimization of stress-induced variations in permeability. Moreover, since the normal incidence component of the magnetic induction is conserved at the defect-steel interface, we examined the flaw geometry effect on the radial MFL profiles for the axially oriented defects. The MFL profiles, in conditions of applied flux density of 1.7 T, for weakly, strongly, and racetrack defects are presented in figure 7, normalized to their respective maximum values.

The wave-like radial MFL profile corresponding to the interacting defects has four extremes, one corresponding to each defect-steel boundary. Accordingly, the MFL profile for the racetrack defect has only two extreme values. For the interacting holes, the overall MFL amplitude of a profile is dictated by the extreme values of the profile corresponding to the "outside" defect edges. The "inside" hole edges, generate smaller amplitude signals, as the critical area between defects is exposed to lower-than-background magnetic flux.

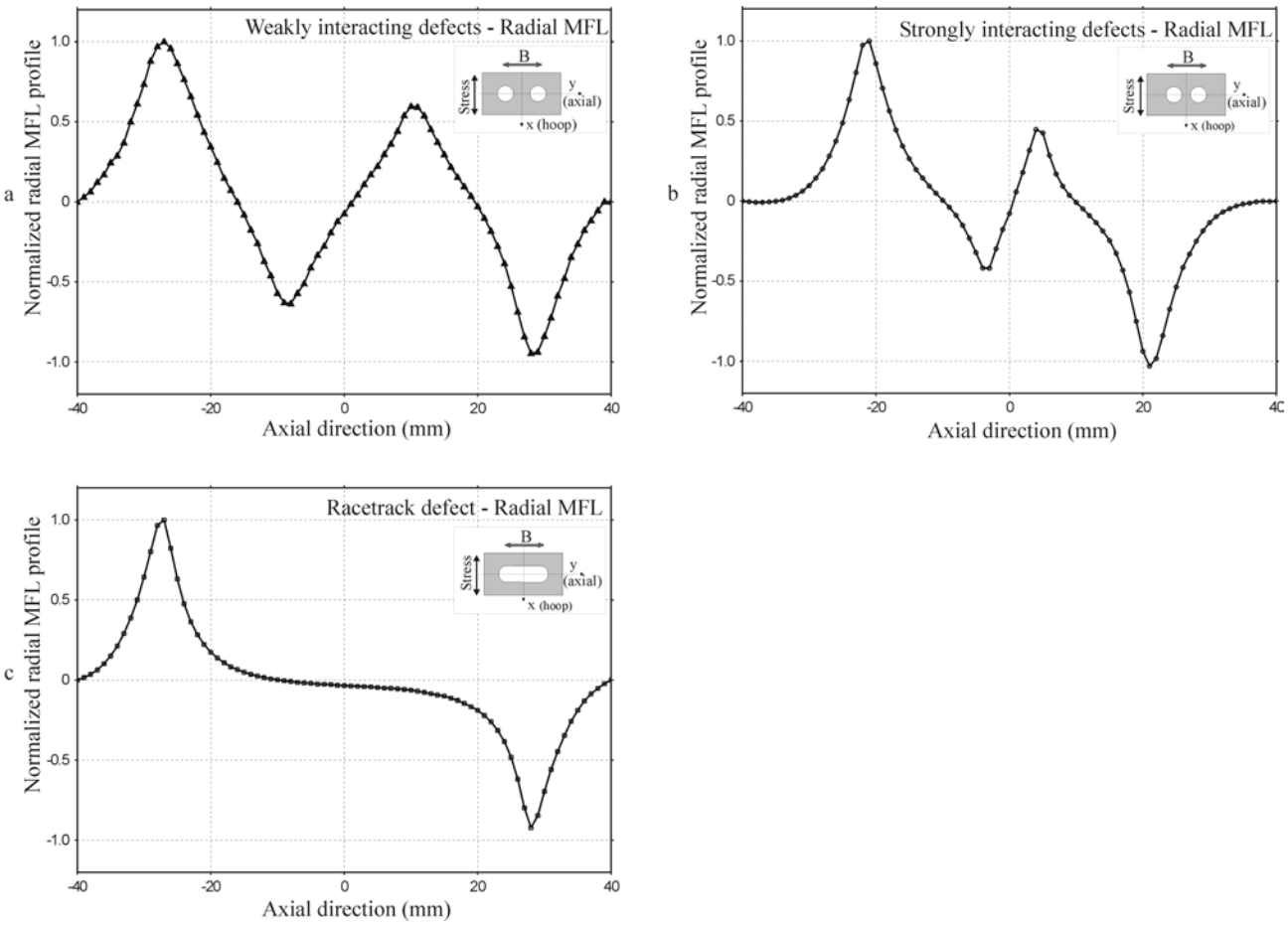

In order to discriminate between stress and defect shielding effects in the area between the interacting defects, the ratio of the intermediary peak amplitude (MFL_{pp} determined from the 2nd and 3rd extreme values) to the overall MFL_{pp} amplitude (determined from 1st and 4th extreme values) is plotted versus applied stress for the axially aligned interacting defects, as shown in figure 8.

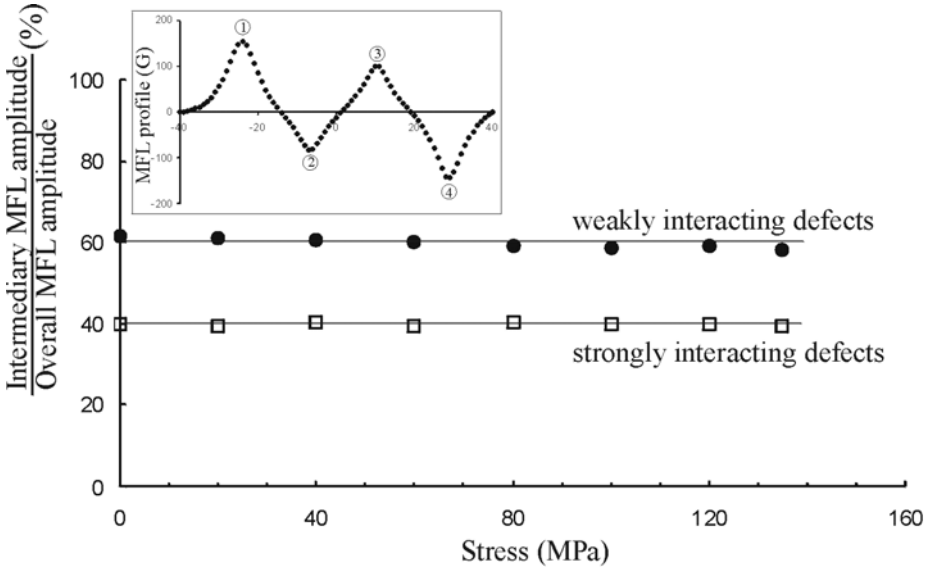

It can be observed from figure 8 that this ratio is independent of the applied stress, and depends only on the separation between the holes. For weakly interacting defects the ratio of intermediary to overall radial MFL_{pp} is about 60%, while for strongly interacting defects the corresponding value is approximately 40%. This consistency suggests that the magnetic shielding provided by the two holes dominates over stress effects in the critical area between defects. This result is somehow unpredicted; since less magnetic flux enters the area between defects, more stress sensitivity was expected for the intermediary peaks of the MFL profile. The plastic deformation may restrict changes in the magnetic permeability in the area between defects.

Conclusion: The experimental results discussed in this study clearly indicate that stress, geometry and magnetic flux density have an effect on the MFL features investigated. As an overall trend, it was observed that the defect-induced MFL_{pp} amplitude decreases with the applied stress, a tendency more pronounced at flux densities away from the saturation level. Circumferential ('hoop') compressive residual stresses developed at the defect edges encouraged an easy axis on the 'axial' direction and higher absolute MFL_{pp}. In the comparison figures 4-6, the general trend was that the larger the residual stress level in the defect vicinities, the larger the MFL_{pp} amplitude. However, this effect is relatively small comparative to the that of bulk elastic stress when the percentage change of the MFL signal, $MFL_{pp}(\%)$, was investigated, especially at low flux density (figure 3.a).

References:

1. L. Clapham, D.L. Atherton, *Magnetic flux leakage inspection of oil and gas pipelines*, Proceedings of the International Symposium on Materials for Resource Recovery and Transport, Calgary, Alberta, Canada, pp. 313-326, 1998;
2. A. Plotnikov, L. Clapham, *Stress effects and magnetic NDE methods for pipeline inspection: a study of interacting defects*, Insight, Vol. 44, No. 2, pp. 74-78, 2002;
3. P. Laursen, D.L. Atherton, *Effects of line pressure stress on magnetic flux leakage patterns*, The British Journal of Non-destructive Testing, Vol. 34, No. 6, pp. 285-288, 1992;
4. R.C. Juvinall, *Engineering Considerations of Stress, Strain, and Strength*, McGraw-Hill Book Company, New York, 1967;
5. D. Roylance, *Mechanics of Materials*, John Wiley & Sons, Inc., New York, 1996;
6. C. Mandache, PhD thesis: *Magnetic Flux Leakage Investigation of Interacting Defects – Stress and Geometry Effects*, Queen's University, Kingston, Ontario, Canada, 2004;
7. L. Clapham, D.L. Atherton, *Stress effects on MFL signals*, Proceedings of Corrosion 2002 Conference, paper 02079, Denver, USA, 2002;
8. P. Ivanov, L. Udpa, *Effects of stress on the probability of detection for magnetic flux leakage inspection*, Review of Progress in Quantitative Nondestructive Evaluation, Vol. 18, Ed. Thompson and Chimenti, Kluwer Academic/Plenum Publishers, pp. 2319-2327, 1999;